Interaction Effects in Conductivity of Si Inversion Layers at Intermediate Temperatures

V. M. Pudalov[a,b], M. E. Gershenson[a], H. Kojima[a], G. Brunthaler[c], A. Prinz[c], and G. Bauer[c]

[a] *Serin Physics Lab, Rutgers University, Piscataway NJ-08854, USA*
[b] *P. N. Lebedev Physics Institute, 119991 Moscow, Russia*
[c] *Johannes Kepler Universität, Linz, A-4040, Austria*

We compare the temperature dependence of resistivity $\rho(T)$ of Si MOSFETs with the recent theory by Zala et al. This comparison does not involve any fitting parameters: the effective mass m^* and g^*-factor for mobile electrons have been found independently. An anomalous increase of ρ with temperature, which has been considered a signature of the "metallic" state, can be described quantitatively by the interaction effects in the ballistic regime. The in-plane magnetoresistance $\rho(B_\parallel)$ is qualitatively consistent with the theory; however, the lack of quantitative agreement indicates that the magnetoresistance is more susceptible to the sample-specific effects than $\rho(T)$.

71.30.+h, 73.40.Qv, 71.27.+a

The theory of quantum corrections due to single-particle (weak localization) and interaction effects has been very successful in describing the low-temperature electron transport in low-dimensional conductors (see, e.g., [1]). There was, however, a noticeable exception: the temperature- and magnetic-field dependences of the resistivity ρ of the most ubiquitous two-dimensional (2D) system, electrons in silicon MOSFETs, defied the theoretical predictions. Serious quantitative discrepancies between the experimental data and the theory of interaction corrections were noticed two decades ago (see, e.g., [2–4]). The gap between the expected and observed low-temperature behavior of ρ became dramatic with the advent of high-mobility Si devices [5]. Despite the earlier attempts to attribute the "anomalous metallic behavior" to the density- and temperature-dependent screening [6], the low-temperature transport in Si MOSFETs [7], as well as other 2D systems with a low carrier density n, resisted explanation for a decade (for reviews, see [8,9]).

Recently, important progress has been made in both experiment and theory, which allows to solve this long-standing problem. Firstly, it has been recognized that multiple valleys in Si MOSFETs enhance interaction effects [10,11]. Secondly, the theory of interaction corrections to the conductivity has been extended beyond the diffusive regime [11]. This development is crucial because the most pronounced increase of ρ with temperature is observed in the ballistic regime (see below). Thirdly, the Fermi-liquid interaction parameters for a dilute electron system in Si MOSFETs have been found from detailed measurements of Shubnikov-de Haas oscillations [12,13]. All this allows to compare the experimental data with the theory [11] without any adjustable parameters.

In this Letter, we show that the most prominent features of the "metallic" state in Si MOSFETs, the strong temperature and in-plane magnetic field dependences $\rho(T)$ and $\rho(B_\parallel)$ at relatively small resistivities $\rho \ll h/e^2$, can be accounted for by the theory [11] over a wide range of carrier densities, temperatures, and magnetic fields. Thus, the "metallic" conductivity of high-mobility Si MOSFETs, which was considered anomalous for a decade, can now be explained by the interaction effects in a system with a large pseudo-spin (two valleys + two spins), and an interaction-enhanced spin susceptibility. Though the theory [11] accounts only for small corrections, it works surprisingly well for some samples even at relatively high temperatures, where $\delta\rho/\rho \sim 1$. The theory, however, does not agree with experiment at very low temperatures and in strong magnetic fields $B_\parallel \gg T/g\mu_B$, as well as at low electron densities, where sample-specific effects come into play [14].

The ac (13 Hz) measurements of the dependences $\rho(T)$ and $\rho(B_\parallel)$ have been performed on six (100) Si-MOS samples from different wafers: Si15 (peak mobility $\mu^{peak} = 4.0\,\mathrm{m^2/Vs}$), Si2Ni ($3.4\,\mathrm{m^2/Vs}$), Si22 ($3.3\,\mathrm{m^2/Vs}$), Si6-14 ($2.4\,\mathrm{m^2/Vs}$), Si43 ($1.96\,\mathrm{m^2/Vs}$), and Si46 ($0.15\,\mathrm{m^2/Vs}$); more detailed description of the samples can be found in Refs. [15].

The quantum corrections to the Drude conductivity $\sigma_D = e^2 n\tau/m^*$ (τ is the momentum relaxation time, m^* is the effective mass of carriers) can be expressed (in units of $e^2/\pi\hbar$) as [11,16]:

$$\sigma(T, B_\parallel) - \sigma_D = \delta\sigma_C + 15\delta\sigma_T + 2[(\sigma(E_Z, T) - \sigma(0, T)]$$
$$+ 2[\sigma(\Delta_v, T) - \sigma(0, T)] + [\sigma(E_Z + \Delta_v, T) - \sigma(0, T)]$$
$$+ [\sigma(E_Z - \Delta_v, T) - \sigma(0, T)] + \delta\sigma_{\mathrm{loc}}(T). \qquad (1)$$

Here $\delta\sigma_C = x[1 - \frac{3}{8}f(x)] - \frac{1}{2\pi}\ln(\frac{E_F}{T})$ and $\delta\sigma_T = f_1(F_0^a)x[1 - \frac{3}{8}t(x, F_0^a)] - (1 - f_2(F_0^a))\frac{1}{2\pi}\ln(\frac{E_F}{T})$ are the interaction contributions in the singlet and triplet channels, respectively [17]; $\delta\sigma_{\mathrm{loc}}(T) = \frac{1}{2\pi}\ln(\tau/\tau_\varphi(T))$ is the weak localization contribution. The terms $\sigma(Z, T) - \sigma(0, T)$ reduce the triplet contribution when the Zeeman energy ($Z = E_Z = 2\mu_B B_\parallel$), the valley splitting ($Z = \Delta_v$), or combination of these factors ($Z = E_Z \pm \Delta_v$) exceed the temperature. The prefactor 15 to $\delta\sigma_T$ reflects enhancement of the triplet contribution due to two valleys of the electron spectrum in (100) Si MOS-

FETs [10]. Because of this enhancement, the "negative" correction to the conductivity due to the triplet channel, $d\delta\sigma_T/dT < 0$, overwhelms the "positive" correction due to the singlet channel and weak localization, $d(\delta\sigma_C + \delta\sigma_{\text{loc}})/dT > 0$. The triplet-channel prefactor might be reduced by inter-valley scattering when the relevant scattering time $\tau_v < \hbar/T$. Equation (1) describes the quantum corrections in both diffusive and ballistic regimes; the crossover occurs at $T \approx (1+F_0^a)/(2\pi\tau)$ [11].

The terms in Eq. (1) are functions of $x = T\tau/\hbar$, Z, and F_0^a; their explicit expressions are given in Ref. [11]. The theory [11] considers the Drude resistivity $\rho_D = 1/\sigma_D$ as a parameter and does not describe the density dependence $\rho_D(n)$. We found ρ_D by extrapolation of the linear dependences $\rho(T)$ to $T = 0$; τ was determined from ρ_D using the renormalized effective mass $m^*(n)$ [13]. The Fermi-liquid parameter $F_0^a \equiv F_0^\sigma$ [18], which controls renormalization of the g^*-factor $[g^* = g_b/(1 + F_0^a)$, where $g_b = 2$ for Si], has been experimentally determined from measurements of the Shubnikov-de Haas (SdH) effect [12,13]. Throughout the paper, we accept $\Delta_v = 0$, because small values $\Delta_v < 1$K do not affect the theoretical curves at intermediate temperatures. Thus, one can compare the experiment and the theoretical prediction with no adjustable parameters; such comparison is the main goal of this paper. In this important aspect, our approach differs from the attempts to determine F_0^a for p-type GaAs [19] and Si-MOSFETs [20] by fitting $\rho(T)$ and $\rho(B_\parallel)$ with the theory [11].
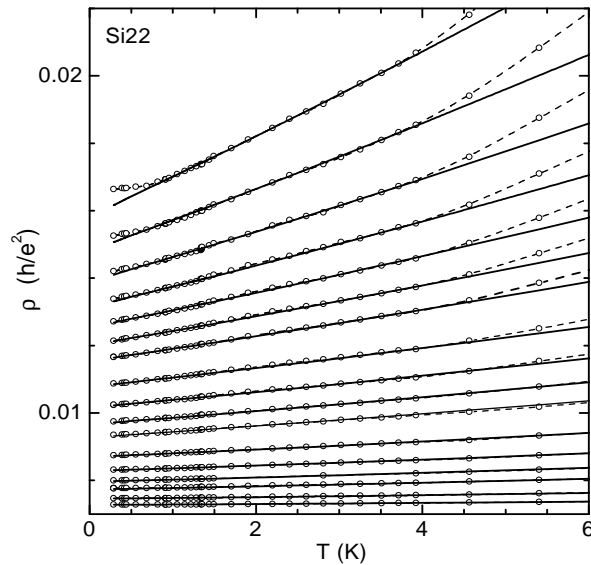

FIG. 1. Resistivity at $B_\parallel = 0$ for sample Si22 vs temperature. The electron densities, from top to bottom are: $n = 5.7, 6.3, 6.9, 7.5, 8.1, 8.7, 9.3, 10.5, 11.7, 12.9, 14.1, 16.5, 18.9, 21.3, 23.7, 28.5, 35.7$ (in units of 10^{11}cm^{-2}). Dots and dashed lines represent the data, solid lines - the theoretical curves with $\Delta_v = 0$ and F_0^a from Ref. [13].

Figure 1 shows the resistivity of sample Si22 versus

temperature for different electron densities. A linear dependence $\rho(T)$ extends over a decade in T, up to $T \approx 0.1E_F$. In this linear regime, the data almost coincide with the theoretical curves (solid lines) calculated with no adjustable parameters. Similar agreement has been observed for samples Si15 and Si43. For the latter sample, the linear $\rho(T)$ dependences remain in agreement with the theory up to such high temperatures ($T \sim 0.3E_F$) that $\delta\rho/\rho \sim 1$ (see Fig. 2). In this case, which is beyond the applicability of the theoretical results [11], we still calculated the corrections to the resistivity according to $\delta\rho = -\delta\sigma\rho_D^2$ [16]. For much more disordered sample Si46, the agreement with the theory is less impressive: the theoretical $\rho(T)$ curves are consistent with the data only at temperatures below 10K, which correspond for this sample mostly to the diffusive regime.
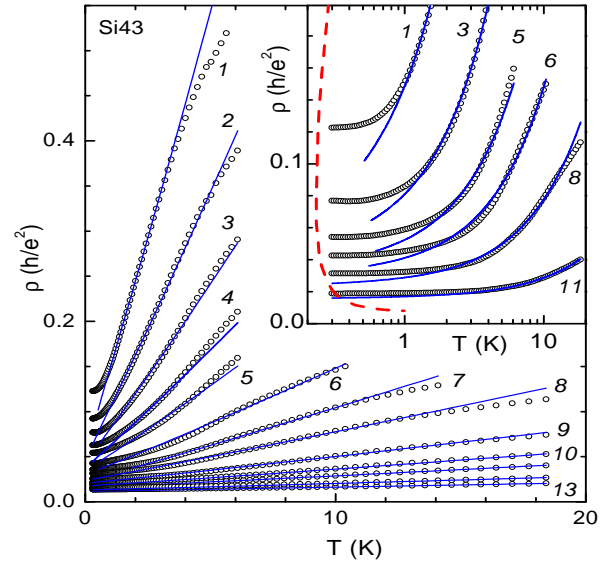

FIG. 2. $\rho(T)$-dependences at $B_\parallel = 0$ for sample Si43 on the linear T-scale (main panel) and logarithmic T-scale (insert). Dots show the data, solid lines correspond to Eq. (1) with $\Delta_v = 0$ and F_0^a from Ref. [13]. The densities are (in units of 10^{11}cm^{-2}): 1 - 1.49, 2 - 1.67, 3 - 1.85, 4 - 2.07, 5 - 2.30, 6 - 2.75, 7 - 3.19, 8 - 3.64, 9 - 4.54, 10 - 5.43, 11 - 6.33, 12 - 8.13, 13 - 9.91. The border between diffusive and ballistic regimes is shown in the inset as the dashed line [11].

For all samples, the data agree with the theory over a broad interval of temperatures (see Figs. 1 and 2), and depart from the theory on both sides of this interval. At high temperature, the $\rho(T)$ data for Si15 and Si22 deviate from the theory up (Fig. 1), while for Si43, they deviate mostly down (Fig. 2). The non-universal deviations indicate the importance of sample-specific localized states at $T \sim E_F$.

On the low-temperature side, the dependences $\rho(T)$ tend to saturate for all samples, in contrast to the theo-

retical prediction Eq. (1). Weakening of the $\rho(T)$ dependence might be caused by a non-zero valley splitting at temperatures $T < \Delta_v$. Indeed, for samples Si22, Si15, and Si6-14, the saturation temperature (0.2 - 0.5 K, see Fig. 1) is of the order of valley splitting estimated from SdH measurements, $\sim (0.6 - 0.8)$K. However, for sample Si43, the saturation temperature is too high (1–8 K, depending on the density - see Fig. 2), which makes this interpretation of the saturation dubious. It is also unlikely that the saturation at such high temperatures could be caused by electron overheating. One of the reasons for decrease in the interaction contribution might be a strong (and sample-specific) inter-valley scattering. A theory which takes inter-valley scattering into account is currently unavailable.

Finally, we note that for lower densities and higher resistivities $\rho \sim h/e^2$, the slope $d\rho/dT$ changes sign. This phenomenon, known as "metal-insulator transition in 2D" (2D MIT), can not be accounted for by the theory [11]; the corresponding data for samples Si43 and Si15 across the 2D MIT can be found in Refs. [9,15]. Here we do not discuss this non-universal and sample-dependent regime [14].
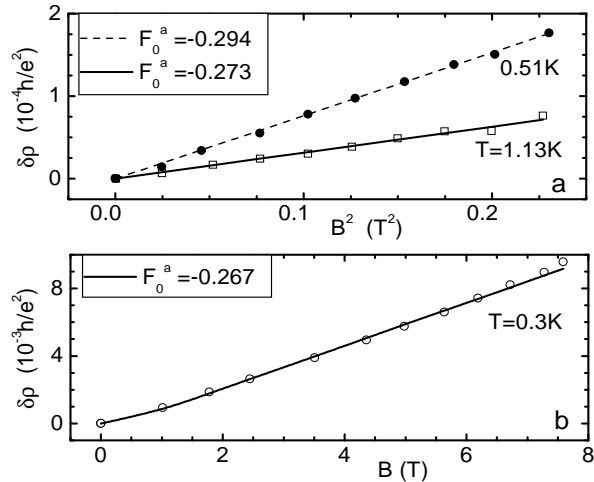

FIG. 3. Magnetoresistivity for sample Si6-14 versus $B_\parallel^2$ at low fields $E_Z/T < 1$ (a), and versus $B_\parallel$ at high fields $E_Z/T \gg 1$ (b). The electron density $n = 4.94 \times 10^{11}$cm^{-2} is the same for both panels. Lines are the best fits with the F_0^a values shown in the panels.

We now turn to the magnetoresistance (MR) data. In contrast to the temperature dependences of ρ, the magnetoresistance agrees with the theory [11] only qualitatively. For this reason, in fitting the experimental data, we treated F_0^a as an adjustable parameter.

Figure 3 shows that the F_0^a values, found for sample Si6-14 from fitting at low ($E_Z/2T < 1$) and high ($E_Z/2T \gg 1$) fields, agree with each other within 10%; at the same time, these values differ by 30% from the values determined in SdH studies [13]. A similar situation

is observed for sample Si43 in weak and moderate fields (Fig. 4c,f and Fig. 4b,e, respectively). The weak systematic decrease of $|F_0^a|$ with $B_\parallel$ in this field range (Figs. 4) agrees qualitatively with non-linearity of magnetization which we observed in SdH measurements [13].

Fitting the weak-field MR at different temperatures provides a T-dependent F_0^a (Fig. 3a). On the other hand, our SdH data for the same sample do not confirm such a dependence: $g^* m^*$ is constant within 2-3% over the same temperature range [13]. This discrepancy stems from the fact, that, according to our data (see also Ref. [3]), the experimental low-field dependence $\rho(B_\parallel, T) \propto B^2/T^\alpha$ with $\alpha \approx 1$, differs from the theoretical one [Eq. (1)].
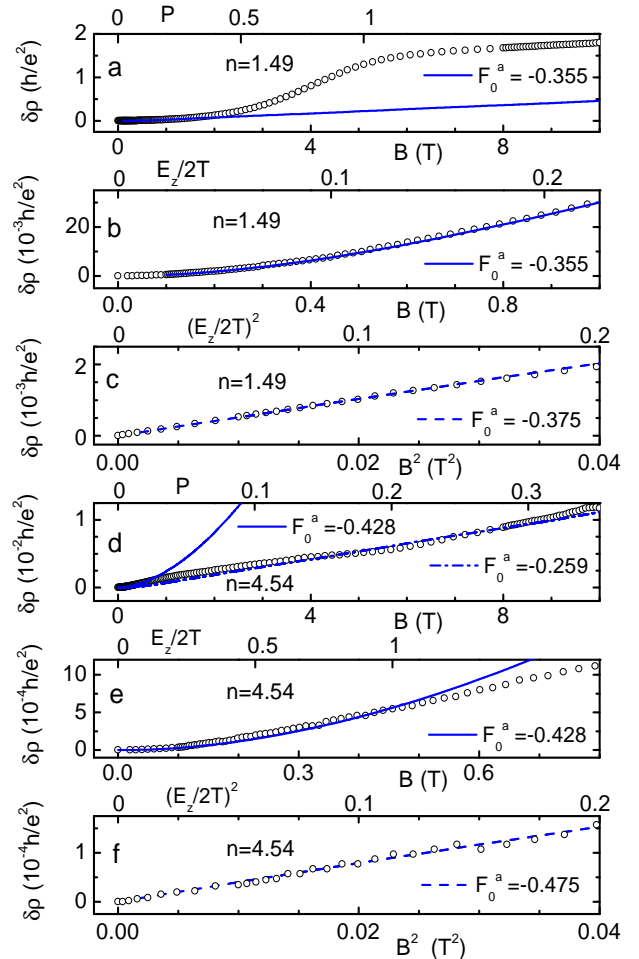

FIG. 4. Magnetoresistivity for sample Si43 vs $B_\parallel$ and $B_\parallel^2$ at $T = 0.3$K for two densities: $n = 1.49 \times 10^{11}$cm^{-2} [panels a, b, c)] and 4.54×10^{11}cm^{-2} [panels d, e, f)]. The upper horizontal scales show $P \equiv g^* \mu_B B_\parallel / 2E_F$ on panels a and d, and $E_Z/2T$ on panels b, c, e, and f.

The discrepancy between the theory and the MR data is much more pronounced for sample Si43 in strong fields $E_Z/2T \gg 1$, where even the sign of deviations becomes density-dependent (compare Figs. 4a and 4e). The non-universal behavior of the MR has been reported earlier

3

for different samples [15], and even for the same sample cooled down to $4\,\mathrm{K}$ at different fixed values of the gate voltage [14]. The reason for this might be the interaction of mobile electrons with field-dependent and sample-specific localized electron states.

The $F_0^a(n)$ values obtained from fitting the low-field MR for three samples are summarized in Fig. 5a. The non-monotonic density dependence of F_0^a and scattering of data for different samples indicate that the MR is more susceptible to the sample-specific effects than $\rho(T)$. For comparison, we present in Fig. 5b the F_0^a-values obtained from fitting of the $\rho(T)$ data for three samples, where we treated F_0^a as a single adjustable parameter. In contrast to Fig. 5a, there is an excellent agreement between the F_0^a values extracted from SdH measurements and from fitting the $\rho(T)$ dependences; the agreement is observed over a wide density range $n = (1.5 - 40) \times 10^{11} \mathrm{cm}^{-2}$.
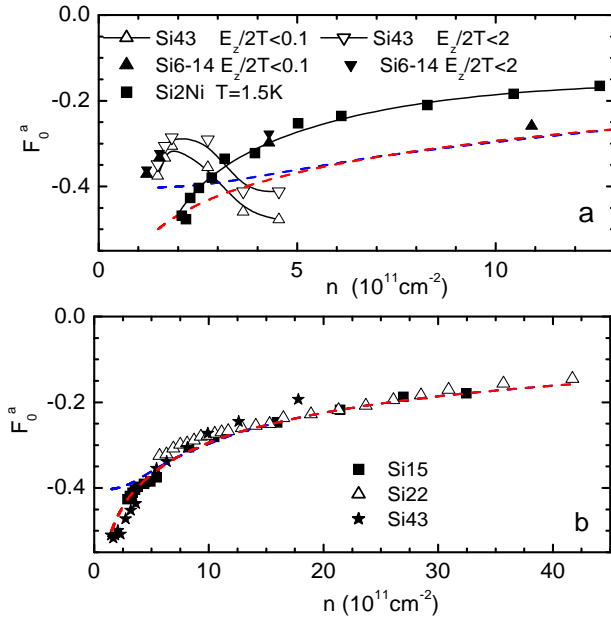

FIG. 5. Comparison of $F_0^a(n)$ values determined from: (a) fitting $\rho(B_\parallel)$ for three samples, and (b) from fitting $\rho(T)$ for three samples. Dashed lines depict upper and lower limits for F_0^a from SdH measurements [13].

In summary, we performed a quantitative comparison of the $\rho(T, n)$ and $\rho(B_\parallel, n)$ data with the theory which accounts for electron-electron interactions [11]. For high-mobility samples, we found an excellent agreement (with no adjustable parameters) between $\rho(T)$ and the theory in the ballistic regime over a wide range of temperatures and electron densities $n = (1.5 - 40) \times 10^{11} \mathrm{cm}^{-2}$. Our experiments strongly support the theory attributing the anomalous "metallic" behavior of high-mobility Si MOSFETs [7] to the interaction effects. Non-universal (sample-dependent) deviations from the theory [11] have been observed (a) at high resistivities $\rho > 0.1 h/e^2$, and

(b) at low resistivities $\rho \ll h/e^2$ for both the lowest temperatures and high temperatures ($T \sim E_F$). The sample-dependent deviations from the theory are more pronounced in the in-plane magnetoresistance, especially in high fields ($2\mu_B B_\parallel / T > 1$). We attribute this non-universality to interaction of the mobile electrons with field-affected localized electron states.

[1] B. L. Altshuler, A. G. Aronov, P. Lee Phys. Rev. Lett. **44**, 1288 (1980).
[2] D. J. Bishop, R. C. Dynes, and D. C. Tsui, Phys. Rev. B **26**, 773 (1982).
[3] V. T. Dolgopolov, S. I. Dorozhkin, and A. A. Shashkin, Solid State Commun. **50**, 273 (1984).
[4] M. S. Burdis and C. C. Dean, Phys. Rev. B **38**, 3269 (1988).
[5] M. D'Iorio, V. M. Pudalov, and S. G. Semenchinsky, Phys. Lett A **150**, 422 (1990).
[6] F. Stern, Phys. Rev. Lett. **44**, 1469 (1980). F. Stern, S. Das Sarma, Solid State Electron. **28**, 158 (1985). A. Gold, V. T. Dolgopolov, Phys. Rev. B **33**, 1076 (1986). S. Das Sarma, E. H. Hwang, Phys. Rev. Lett. **83**, 164 (1999).
[7] S. V. Kravchenko, G. V. Kravchenko, J. E. Furneaux, V. M. Pudalov, and M. D'Iorio, Phys. Rev. B **50**, 8039 (1994).
[8] E. Abrahams, S. V. Kravchenko, and M. P. Sarachik, Rev. Mod. Phys. **73**, 251 (2001).
[9] B. L. Altshuler, D. L. Maslov, and V. M. Pudalov Physica E, **9**(2) 209-225 (2001).
[10] A. Punnoose, A. M. Finkelstein, Phys. Rev. Lett. **88**, 016802 (2002).
[11] G. Zala, B. N. Narozhny, and I. L. Aleiner. Phys. Rev. B **64**, 214204 (2001); Phys. Rev. B **65**, 020201 (2001).
[12] T. Okamoto, K. Hosoya, S. Kawaji, and A. Yagi, Phys. Rev. Lett. **82**, 3875 (1999).
[13] V. M. Pudalov, M. Gershenson, H. Kojima, N. Butch, E. M. Dizhur, G. Brunthaler, A. Prinz, and G. Bauer, Phys. Rev. Lett. **88**, 196404 (2002). The upper and lower limits for the g^*-factor over the range $r_s = 1.6 - 8.3$ are: $g^*_{\mathrm{high}} = 2 + 0.3485 r_s - 0.01068 r_s^2 + 0.00048 r_s^3$ and $g^*_{\mathrm{low}} = 2 + 0.1694 r_s + 0.1233 r_s^2 - 0.03107 r_s^3 + 0.002 r_s^4$.
[14] V. M. Pudalov, M. E. Gershenson, H. Kojima, cond-mat/0201001.
[15] M. Pudalov, G. Brunthaler, A. Prinz, G. Bauer, cond-mat/0103087; Phys. Rev. Lett. **88**, 076401 (2002).
[16] I. L. Aleiner, B. N. Narozhny, private communication.
[17] Throughout the paper, we use the unrenormalized Fermi energy E_F.
[18] $F_0^a = -F$, in notations of Refs. [1,2].

[19] Y. Y. Proskuryakov, A. K. Savchenko, S. S. Safonov, M. Pepper, M. Y. Simmons, and D. A. Ritchie, cond-mat/0109261.

[20] A. A. Shashkin, S. V. Kravchenko, V. T. Dolgopolov, T. M. Klapwijk, cond-mat/0111478. S. A. Vitkalov, K. James, B. N. Narozhny, M. P. Sarachik, T. M. Klapwijk, cond-mat/0204566.